INSTITUT DE FRANCE
Académie des sciences

Comptes Rendus
Mécanique

Mohamed Fourati, Zied Kammoun, Jamel Neji and Hichem Smaoui

Large-scale smooth plastic topology optimization using domain decomposition

Volume 349, issue 2 (2021), p. 323-344

Published online: 7 June 2021

https://doi.org/10.5802/crmeca.88

Les Comptes Rendus. Mécanique *sont membres du Centre Mersenne pour l'édition scientifique ouverte*
www.centre-mersenne.org
e-ISSN : 1873-7234

Comptes Rendus
Mécanique
2021, 349, nº 2, p. 323-344
https://doi.org/10.5802/crmeca.88

Short paper / *Note*

Large-scale smooth plastic topology optimization using domain decomposition

Mohamed Fourati [a], **Zied Kammoun** [*, b], **Jamel Neji** [a] **and Hichem Smaoui** [c, a]

[a] Université de Tunis El Manar, Ecole Nationale d'Ingénieurs de Tunis, LR11ES16 Laboratoire de Matériaux, Optimisation et Energie pour la Durabilité, 1002, Tunis, Tunisie

[b] Université de Carthage, Institut Supérieur des Technologies de l'Environnement de l'Urbanisme et du Bâtiment, 2 Rue de l'Artisanat Charguia 2, 2035 Tunis, Tunisie

[c] Faculty of Engineering, King Abdulaziz University, P.O. Box 80230, Jeddah, Kingdom of Saudi Arabia

E-mails: mo_fourati@yahoo.com (M. Fourati), kammounzied@yahoo.fr (Z. Kammoun), jamel.neji@enit.rnu.tn (J. Neji), hismaoui@yahoo.fr (H. Smaoui)

Abstract. A domain decomposition procedure based on overlapping partitions of the design domain is proposed for solving large problems of smooth topology optimization of plastic continua. The procedure enables the solution of problems with sizes exceeding the available computational and storage capacities. It takes advantage of the favorable features of the integrated limit analysis and design formulation of the smooth topology design problem. The integrated approach preserves the mathematical structure and properties of the underlying static, lower bound problem of limit analysis. In particular, the formulation is characterized by weak coupling between subproblems because it does not involve a stress–strain relationship. The decomposition strategy begins by solving a reduced design problem, using a coarse finite element mesh, followed by an iterative process using a fine discretization. At each iteration, an independent topology optimization subproblem is associated with each subdomain, considered as a substructure. The traction vectors acting on the subdomain boundaries are updated at each iteration as the overlapping partitions are switched. The numerical tests showed that as early as the first iteration, the decomposition process generates a feasible, near optimal design with a weight less than 0.1% above the direct solution.

Keywords. Topology optimization, Direct method, Limit analysis, Domain decomposition, Plastic design.

Manuscript received 19th September 2020, revised 17th April 2021, accepted 17th May 2021.

* Corresponding author.

1. Introduction

The topology design of continuum structures of practical significance often requires complex finite element models that lead to large size optimization problems exceeding the available computational and storage capacities. Typical examples of such large problems include the design of three-dimensional (3D) structures [1,2], problems involving multiple geometric scales, and problems dealing with the simultaneous design of material and structure [3, 4]. A variety of strategies known under various designations such as global–local [4], multilevel [5], and decomposition [6–8] have been developed for handling large-scale mathematical problems. These strategies generally consist of splitting the posed problem into a controlled series of smaller problems that can be solved sequentially or in parallel. Many decomposition techniques have been proposed for solving large problems in the topology optimization of elastic structures [3, 4, 9, 10]. However, decomposition schemes for plastic topology design of continua are yet to be developed. This is understandable since design methods that efficiently solve plastic topology optimization problems for continuum structures have appeared only recently [11–17]. The key idea in these methods, which was introduced and detailed in [11], consists of formulating the plastic analysis problem using direct methods to limit analysis [18, 19] and to integrate the analysis and design problems into a single mathematical problem. It was considered for smooth topology design in [11–14] and extended to discrete (i.e., 0–1) design in [16, 17, 20]. Although the discrete design is generally the primary goal, the smooth design problem is worthy of study as it is a component in many solution strategies for discrete design [16,21]. This suggests addressing the treatment of large-scale problems in smooth topology optimizations of plastic media as these large problems would ultimately arise with the growing interest in plastic topology design. Following decades of research, structural topology optimization has reached an advanced stage of development demonstrated by its wide use in the industry. This development has been predominantly focused on the linear elastic behavior, which was paramount for the formulation of the compliance minimization approach [10]. The need for the rigorous fulfillment of strength requirements at the local level furthered the alternative stress-based formulation [22–25]. Both the compliance and stress-based approaches are known for the nonlinear and nonconvex character of the design problem and for the high computational demand due to the repetitive analyses and gradient calculations required in the design process. Sequential convex approximation strategies such as CONLIN, the diagonal SQP [26], and the popular method of moving asymptotes [27] are globally convergent and computationally efficient search methods. Furthermore, the approximate problems involved in these strategies are separable and convex, which is suitable for numerical solution.

These solvers can be applied directly to the smooth topology optimization problem where the pseudo-densities are allowed to take on the range of values between 0 and 1. Numerous difficulties encountered even in smooth topology design, for example, the multiplicity of local minima and the singularity associated with vanishing densities [22], were addressed [23, 28] to improve the robustness of the design methods. In engineering practice, the demand for discrete, that is, 0–1 topology optimization is far more important than for smooth topology. Because of the combinatorial nature of the discrete design problem, the exact methods exhibit nonpolynomial complexity. Therefore, heuristic, for example, evolutionary methods [29] and approximate mathematically based methods [21, 30] were among the alternative strategies used to solve discrete design problems of meaningful size in reasonable times. Moreover, the 0–1 topology optimization problem is known to be ill-posed because the feasible set of the exact (non discretized) problem is not closed [31]. Methods such as the popular Solid Isotropic Material with Penalization (SIMP) [21,32] and the homogenization methods [30] provided effective strategies that typically use continuation schemes [21] involving sequences of smooth design problems. In addition,

they incorporate filtering techniques [33] and geometric constraints [1, 34] to eliminate the checkerboard and mesh dependence phenomena associated with the ill-posedness of the problem. Recently, research in topology optimizations of elastic media is witnessing increased interest in large-scale and multilevel methods [4] as problem complexity and size continue to grow.

In contrast with the tremendous achievements made in the framework of elastic design, research work on the topology optimization of plastic continua is limited because of the complexity and the high computational demand of analyses and sensitivity calculations involving plastic behavior. Typically, the nonlinear analysis is performed using incremental procedures [35] that follow the evolution of the response throughout the loading path. The topology optimization is often carried out using methodologies developed for linear elastic problems and adapted to deal with the difficulties associated with the material and geometric nonlinearities [36], for example, the path-dependence of the response sensitivity [37]. Apart from a few exceptions, for example, [36], contributions involving elastoplastic materials are restricted to infinitesimal strains.

In many engineering problems, the information on the history of the response is unnecessary. Ultimate limit state design in geotechnical and structural engineering are typical examples where only the limit state is of interest [38]. Limit analysis (LA), also known as yield design [38], specifically provides a direct approach for determining the limit state in terms of the plastic collapse load and stress distribution, or velocity fields, under the assumption of infinitesimal strain. The theory of limit analysis is based on the fundamental lower bound and upper bound theorems [39] originally presented by [40]. Finite element formulations of limit analysis for planar continua were proposed in [41, 42], where the LA problem takes the form of a numerical mathematical programming problem. The latter is linearly constrained except for the yield constraints. In the early works, the convex yield criterion was approximated in a piecewise linear form so that the LA problem could be solved using linear [43] or quadratic programming [41]. The subsequent developments in mathematical programming provided solvers (e.g., [44]) that can handle static [45–49] and kinematic [19, 46, 50] numerical problems of LA involving more complex yield criteria.

Limit analysis was applied in [11] in the context of smooth plastic topology optimization of continua by adopting a stress-based integrated analysis and design approach [6]. The design problem was formulated as a single mathematical problem by augmenting the static lower bound problem of limit analysis with the material densities representing the design variables while the nodal stresses were treated as independent response variables.

As a result, the design problem preserves the bulk of the mathematical structure and properties of the LA problem, especially convexity, the conic quadratic programming form, and the rigorous lower (or upper) bound character of the solution. These properties were found to convey attractive characteristics to the solution process, such as mesh independence and near-linear time complexity [11, 14]. Moreover, limit analysis does not require a behavior law, which weakens the coupling between subproblems in a decomposition context. The concept of integrated limit analysis and design was pivotal to a number of subsequent studies dealing with smooth [12–14] and discrete [16, 17, 20] topology design of plastic continua.

The integrated analysis and design strategy was applied in nonlinear elastic design [51, 52] to replace the nested nonlinear analysis and optimization problems with a single nonlinear programming problem. This resulted in excessively large optimization problems where the nonlinear analysis equations were included as equality constraints, and the kinematic response quantities, for example, the displacements, were treated as independent variables. These constraints create a strong coupling that is unsuitable for decomposition. In [6], the integrated approach was applied to the plastic design of trusses, frames, and shear panels based on limit analysis, and a decomposition was proposed to solve the large optimization problem. Because of the weak coupling between substructures in the absence of behavior law, the block separable structure of the

mathematical optimization problem was suitably tailored for decomposition according to the Dantzig–Wolfe scheme, also known as the column generation method [8, 53].

Decomposition techniques are diverse and abundant in the literature. Methods that are governed by mathematical considerations exploit specific features in the algebraic structure of the mathematical problem that enable solutions using established decomposition algorithms. The Dantzig–Wolfe decomposition [53] and its dual counterpart Benders' decomposition [8, 54] are classical examples in this category. Other methods are based on physical grounds wherein the physical system is divided into subsystems described by smaller problems or subproblems. In the iterative approach, the coupled subproblems are solved separately through an iterative process where interface parameters are repeatedly updated [10]. Another approach based on physics is substructuring. Originally developed in the context of structural analysis, it was also employed in multilevel structural optimization [5]. The subsystems, that is, the substructures, are treated as superelements, and a global system of reduced dimension associated with the interface degrees of freedom is formed through static condensation [7].

A variety of decomposition approaches have been developed for topology optimization of elastic continua. Domain decomposition was applied to topology designs of two-dimensional (2D) [10] and 3D [9] continua for minimum compliance using a parallel preconditioned conjugate gradient algorithm for analysis and sensitivity calculations. In [9], parallel computing was also applied to the method of moving asymptotes [27]. Two-scale (macro and micro) computational procedures were developed for simultaneous topology design of the structure and the material in [3]. The decomposition was carried out with respect to the macroscale finite elements, which play the role of subdomains, and the associated local optimization problems were solved in parallel. In [4], a general framework is proposed for the simultaneous design of the structure and the composite material in a multi-scale optimization strategy that accounts for the fully detailed description and behavior of the composite material at the relevant scale. While this strategy was illustrated in a sizing design framework, the concept can be extended to topology optimization. Multigrid methods [33, 55] employ a hierarchy of nested domain partitions and a strategy of transfer of information between levels. The sequencing of coarse and fine domain partitions and the associated transfer operators enable to capture both the low- and high-frequency components in the errors on the stress field.

The approach presented in [6] is a rare example of decomposition in plastic design. Although it was applied to sizing type problems, the Dantzig–Wolfe method is directly extendable to the smooth topology optimization of continua using the integrated limit analysis and design concept. The Dantzig–Wolfe algorithm is known to have a finite but rather slow convergence, and its complexity depends on the algorithms used in solving the master problem and the subproblems. Therefore, reconsidering the method in light of the recent progress in mathematical programming is a pertinent subject of investigation. An alternative direction to explore is decomposition based on the division of the physical domain. Interestingly, an effective domain decomposition strategy was proposed for the kinematic [56] and the static [47] problems of LA in plane strain and was extended to the static problem in three dimensions in [57]. In plane problems it involves two overlapping partitions of the domain. At each step of decomposition, one of the partitions is used, and an independent limit analysis subproblem is associated with each subdomain, considered as a substructure.

The similarity of the LA-based plastic design problem and the underlying LA problem suggests that the decomposition paradigm should hold for the former with comparable performance. In the present work, the domain decomposition technique, proposed in [47] for large-scale LA, is extended to perform smooth topology optimization of plastic continua with large problem sizes.

The paper is structured as follows: the static method of limit analysis is presented, and the mathematical formulation of the finite element limit static analysis problem is formulated in

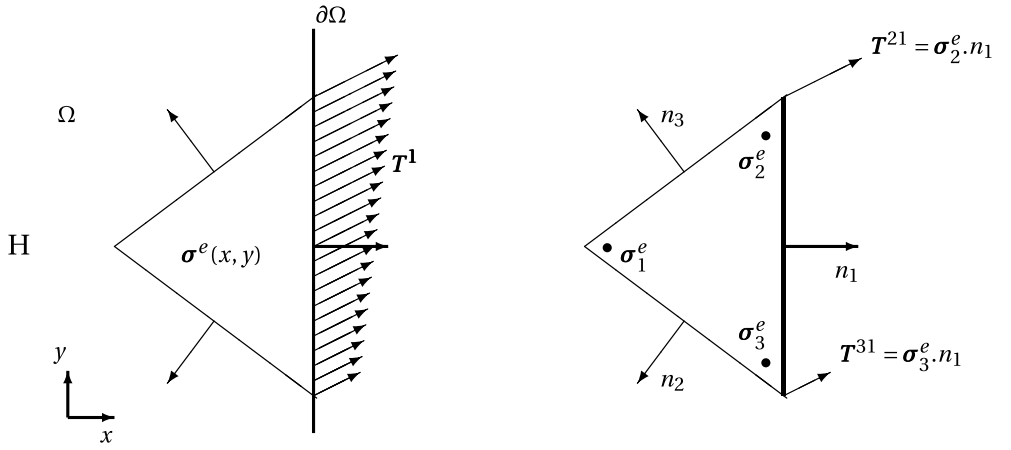

a) Element stress field

b) Nodal stresses and traction vectors

Figure 1. The three-node triangular element.

Section 2. Then the smooth plastic topology optimization problem is defined, and its mathematical formulation is given in Section 3. In Section 4, the proposed domain decomposition is described and justified. Then in Section 5, the results of a series of numerical examples treated using the decomposition procedure are presented and discussed. Finally, Section 6 is dedicated to concluding remarks.

2. Formulation of the static lower bound problem

Let Ω denote a mechanical domain and $\partial\Omega$ its boundary, represented in the Cartesian coordinates (x, y). The domain is supported at a subset $\partial\Omega_s$ of $\partial\Omega$, and a loading system $\boldsymbol{T}$ is prescribed on the unrestrained boundary $\partial\Omega_T$. The unloaded boundary will be denoted by $\partial\Omega_0$. The weightless material is governed by a Tresca plasticity criterion, and the strain is assumed to be infinitesimal.

Adopting the terminology defined in [58], a stress field $\boldsymbol{\sigma}$ is said to be statically admissible if it satisfies the field equilibrium equations in Ω, the continuity of the stress vector on any existing internal discontinuity lines, and the stress boundary conditions on $\partial\Omega_{\boldsymbol{T}}$. It is termed plastically admissible if it satisfies the plasticity criterion in all Ω. A stress field will be said to be admissible if it is both statically and plastically admissible. A loading is statically admissible (respectively, admissible) if it is in equilibrium with a statically admissible (respectively, admissible) stress field.

According to the lower bound theorem, for a proportional loading system, the static (lower bound) problem of limit analysis consists of finding the collapse load defined by the maximum loading parameter λ such that the loading $\lambda\,\boldsymbol{T}$ is in equilibrium with a statically and plastically admissible stress field. Clearly, the only physical response quantities involved in the formulation are the stresses. The displacements or velocities can be interpreted as dual variables in the dual problem, which is an expression of the kinematic (upper bound) problem of limit analysis.

Owing to the convexity of the yield criterion and the linearity of the static admissibility conditions, the static lower bound problem is convex. Hence, any load that is in equilibrium with a feasible stress field constitutes a rigorous lower bound for the collapse load. In particular, this holds for feasible stress fields generated using finite elements. In the present plane strain formulation, the stress field is modeled using the finite element discretization presented in detail in [43] and described in Figure 1.

The domain is divided into a uniform mesh of triangular finite elements with nodes located at the vertices. The element stress field $\boldsymbol{\sigma}$ is interpolated linearly [43] from the nodal stress tensors $\boldsymbol{\sigma}_1^e$, $\boldsymbol{\sigma}_3^e$, and $\boldsymbol{\sigma}_3^e$. At a given node, an independent nodal stress tensor is assigned to each element sharing the same node since continuity across element boundaries is required solely for the traction vector. A statically admissible stress field should satisfy the field equilibrium equations

$$\operatorname{div}(\boldsymbol{\sigma}) = 0 \tag{1}$$

within each element. It should also satisfy the boundary conditions on the traction vector

$$\boldsymbol{\sigma} \cdot n = \boldsymbol{T} \tag{2}$$

at the nodes of each unrestrained side of each element, $\boldsymbol{T}$ representing the prescribed nodal stress vector acting on the element side with unit normal vector n. In addition, the traction vector continuity conditions

$$(\boldsymbol{\sigma}^{e_1} - \boldsymbol{\sigma}^{e_2}) \cdot n = 0 \tag{3}$$

should be verified at the ends of the interelement boundary between each pair of elements (e_1, e_2). The linear interpolation implies that conditions (2) and (3) are satisfied along the element side. Therefore, Equations (1)–(3) are also sufficient conditions for the stress field to be statically admissible. Furthermore, Equations (1)–(3) are linear in the stress variables and can be written in the form

$$[\mathbf{A}]\ \{\sigma\} = \{T\}, \tag{4}$$

where $\{\sigma\}$ is a vector collecting the components of all the nodal stress tensors, and $\{T\}$ a force vector assembling the right-hand side components of (1)–(3). These force components consist of either nodal boundary tractions or zeroes. In plane strain, the Tresca plasticity criterion is expressed as

$$S(\boldsymbol{\sigma}) = \sqrt{\left(\frac{\sigma_{xx} - \sigma_{yy}}{2}\right)^2 + \tau_{xy}^2} \leq \bar{s}, \tag{5}$$

where $\bar{s}$ denotes the shear strength of the material. Because the criterion is convex and the element stress fields are linear, satisfying the criterion at the nodes implies that it is verified inside the elements. Thus, it is sufficient to impose (5) on the nodes for plastic admissibility of the element stress field.

The numerical static lower bound problem of limit analysis can be expressed in the following convex programming problem form

$$\begin{aligned} &\max_{\lambda,\boldsymbol{\sigma}} \lambda \\ &\quad [\mathbf{A}]\{\sigma\} = \lambda\{T\}, \\ &\quad S(\boldsymbol{\sigma}) \leq \bar{s} \quad \text{at all nodes.} \end{aligned} \tag{6}$$

Applying the variable change $\sigma^+ = (\sigma_{xx} + \sigma_{yy})/2$, $\sigma^- = (\sigma_{xx} - \sigma_{yy})/2$, the criterion can be cast in the conic form $\sigma^{-2} + \tau^2 \leq \bar{s}^2$. This transforms the limit analysis problem into a conic quadratic programming problem [44, 59], which can be solved efficiently using the conic programming module in Mosek [60] based on an interior point method.

3. The plastic topology optimization problem

The plastic topology design problem considered here consists of finding the optimal distribution of material in a rectangular domain Ω such that the amount (e.g., weight) of material be minimum while the specified supported load $\boldsymbol{T}$ remains statically and plastically admissible. The material distribution is described by a pseudo-density field ρ with values ranging between

zero (void) and unity (the natural material). In a finite element formulation of the problem, the domain is discretized into a uniform grid of $n_x \times n_y$ rectangles, diagonally subdivided into four triangular finite elements each. For the sake of simplicity, a uniform density will be adopted within the element.

As detailed in [11], the smooth topology design problem can be derived from the limit analysis problem (6) through the following modifications. First, the load parameter λ is set to unity while the element material densities are treated as independent design variable together with the nodal stresses. A continuation scheme is adopted that relates the shear strength s to the density by $s = \rho\bar{s}$. Finally, additional simple linear constraints are imposed on the trace σ^+ of the stress tensor to prevent the artificial formation of pressure traps [11]. These are void regions that appear where the criterion may be satisfied with zero shear strength while the spherical stress can be finite. The resulting integrated analysis and design problem is expressed in the form of a conic quadratic programming problem, denoted by (P)

$$\begin{aligned} \min_{\rho,\boldsymbol{\sigma}} \int_\Omega \rho \, \mathrm{d}\Omega \\ [\boldsymbol{A}]\{\sigma\} = \{T\}, \\ S(\boldsymbol{\sigma}) \le \rho\bar{s} \quad \text{at all nodes}, \\ \sigma^+ \le K\rho \quad \text{at all nodes}, \\ \rho \in [0,1], \end{aligned} \tag{7}$$

where K is a constant coefficient set to 10. This value was recommended in [11] based on an investigation showing that the accuracy of the optimum solution was satisfactory and practically insensitive to K for values of 10 and higher.

The problem P shares many of the appealing properties of the underlying limit analysis problem. In addition to being convex and node-wise separable in the stress variables, it is linear with respect to the densities. All the problem functions and gradients are simple and explicit analytical expressions of the densities and nodal stresses. The gradients of the linear constraints, expressed by the coefficient matrix $[A]$, are constant and sparse. The problem exhibits the same desirable properties of the approximate problems employed in sequential convex programming. Therefore, the conic programming solver operates directly on the "exact" optimization problem without resorting to approximate programming.

Furthermore, the lower bound property of the LA problem proves to be useful for comparing and measuring the accuracy of the solutions to the design problem. It implies that the optimum solution of problem P is a conservative design with respect to the "exact" design problem. In fact, any feasible solution to problem P corresponds to an upper bound for its optimal value. Consider a hierarchy of design problems generated from the finite element models such that for any pair of these models, any element in the coarser mesh is a partition of elements of the finer one. The optimal weights relative to a sequence of increasingly fine models form a decreasing sequence. Using the default tolerance of 10^{-6} on the absolute constraint violations [60], the numerical optimization errors can be neglected, and the weight can serve as a measure of the accuracy of the finite element discretization.

4. Domain decomposition of the design problem

The purpose of the decomposition is to replace the mathematical optimization problem associated with the $n_x \times n_y$ mesh referred to as the "target mesh" by a family of problems of smaller size. In the proposed domain decomposition, these problems, or subproblems, are topology optimization problems associated with finite element models that are smaller than the target model. Consider the topology design problem P (7), formulated based on the target mesh, as the "target problem".

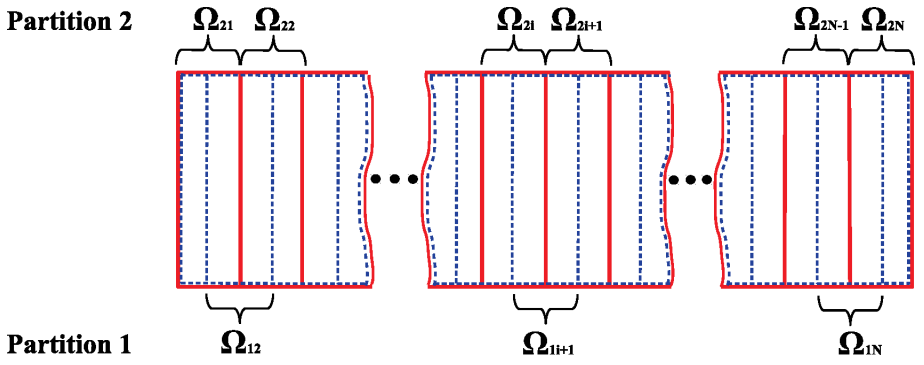

Figure 2. The two partitions of the domain.

To carry out the decomposition, the design domain Ω is subdivided as detailed in [47] into an overlapping pair of partitions (Figure 2), one of $N-1$ subdomains, denoted by $\Omega_{1i},\ i=2,\dots,N$, and another of N subdomains, denoted by $\Omega_{2i},\ i=1,\dots,N$.

For the sake of clarity, the domain is divided serially across a single direction, which makes the presentation and the indexing simple without loss of generality. The boundary of a subdomain Ω_{pi} is composed of the boundary $\partial\Omega_{T'_{pi}}$ it shares with neighboring subdomains and a part, $\partial\Omega_{T_{pi}} \cup \partial\Omega_{0_{pi}}$, of the external boundary of the domain. Each subdomain Ω_{pi} is considered as a substructure subject to a loading $\boldsymbol{T}_{pi}$ defined by the restriction of the prescribed load $\boldsymbol{T}$ to the subdomain external boundary $\partial\Omega_{T_{pi}}$ and the variable traction vectors $\boldsymbol{T}'_{pi}$ acting on the internal boundary $\partial\Omega_{T'_{pi}}$ shared with neighboring subdomains.

Each subdomain shares with its neighbors one or more internal boundaries, where the traction vector continuity condition (3) involves stress variables associated with the neighbors. In fact, these conditions are the only source of coupling among the subdomains. In order to express each subproblem exclusively in terms of its own variables, we will introduce new variables z and replace (3) with an equivalent pair of equations

$$\boldsymbol{\sigma}^{e_1} \cdot n = z, \quad \boldsymbol{\sigma}^{e_2} \cdot n = z, \tag{8}$$

where the elements e_1 and e_2 belong to different subdomains and z clearly represents the nodal traction vector, denoted by T', at the common boundary. This modification transforms the problem P into an equivalent problem P', where the internal tractions are independent variables. It is important to note that if the internal tractions $\boldsymbol{T}'_{pi}$ is deliberately fixed, the coupling among the subdomains is eliminated, and solving the modified problem P, that is, P', becomes equivalent to solving a set of independent subproblems.

Let a topology design problem (P_{pi}), similar in form to problem P, be posed for each subdomain Ω_{pi} as follows:

$$\begin{aligned}
&\min_{\rho,\boldsymbol{\sigma}} \int_{\Omega_{pi}} \rho \,\mathrm{d}\Omega \\
&\begin{bmatrix} \boldsymbol{A}_{pi} \\ \boldsymbol{A}'_{pi} \end{bmatrix} \{\sigma\} = \begin{Bmatrix} T_{pi} \\ T'_{pi} \end{Bmatrix}, \\
&S(\boldsymbol{\sigma}) \le \rho \bar{s} \quad \text{at all nodes in } \Omega_{pi}, \\
&\sigma^+ \le K\rho \quad \text{at all nodes in } \Omega_{pi}, \\
&\rho \in [0,1],
\end{aligned} \tag{9}$$

where ρ and $\boldsymbol{\sigma}$ are restrictions of the density and stress fields to Ω_{pi}.

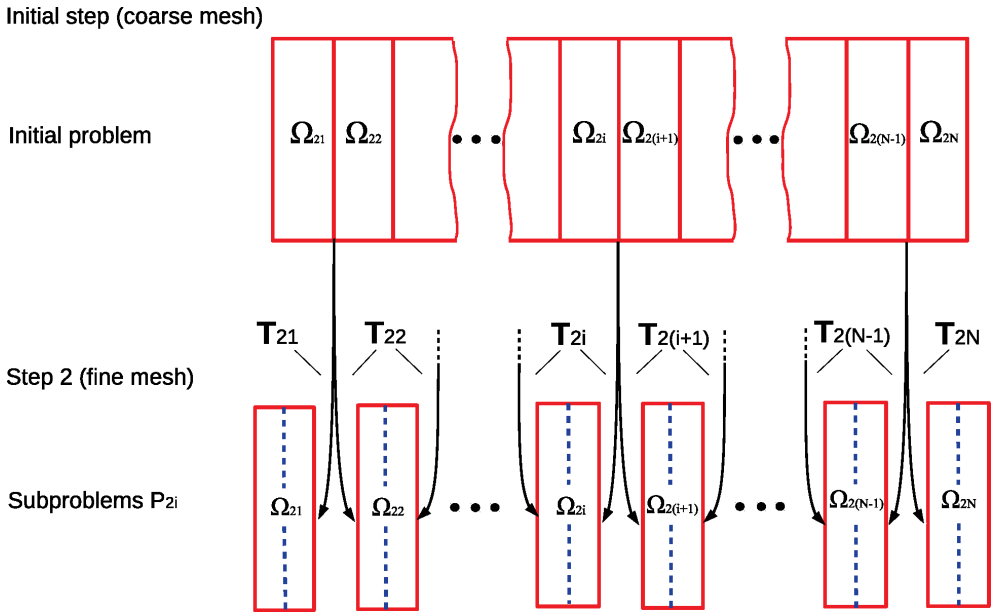

Figure 3. Decomposition flow diagram—the first iteration.

The decomposition strategy consists of a sequence of iterations, each comprising two steps that are identical except for the first iteration. The initial step of the first iteration (Figure 3) provides a starting approximate solution to problem P by solving a coarse mesh problem (e.g., $n_x/2 \times n_y/2$), called the "initial problem" and denoted by (P_1), of sufficiently small size to enable solvability. The finite element meshes are designed such that any element in the coarse model is the union of elements in the target model to ensure that any feasible solution for the initial problem is also feasible for the target problem and the subproblems.

The solution of problem P_1 provides a feasible solution with a reduced weight and an initial admissible stress field, including the nodal traction vectors at the subdomain interfaces. In the following steps, all subproblems will be based on the discretization relative to the "target mesh". This requires the evaluation of the stresses at the internal boundary nodes not existing in the coarse mesh in order to construct the loading vectors $\boldsymbol{T}'_{pi}$. For the first iteration, the construction of $\boldsymbol{T}'_{2i}$ to be used in the second step is completed through linear interpolation.

In the second step of the first iteration, the design subproblems P_{2i} relative to the subdomains Ω_{2i} subject to the fixed loads $\boldsymbol{T}'_{2i}$ are solved independently. Their collective result constitutes a feasible approximate solution $(\rho, \boldsymbol{\sigma})$ to the design problem P over the entire domain Ω with an updated weight that should be lower than or equal to the value in Step 1.

In addition, a new family of traction vectors $\boldsymbol{T}'_{1i}$ is derived from the new stress field evaluated at the interior of the subdomain. These tractions $\boldsymbol{T}'_{1i}$ will serve as a prescribed loading in the subsequent family of subproblems P_{1i}. Because of the overlapping of the two sets of subdomains, the interface between any pair of subdomains is located at the interior of a subdomain in the other set. This allows an update of the stresses on a given interface at every other step.

The following iterations, starting with iteration 2 (Figure 4), are all similar. They begin with Step 1, where the subproblems P_{1i} associated with the subdomains Ω_{1i} are solved using the updated loads $\boldsymbol{T}'_{1i}$. Their solutions provide an improved design with a reduced weight and the updated load vectors $\boldsymbol{T}'_{2i}$. Step 2 is identical to the second step of the first iteration described above.

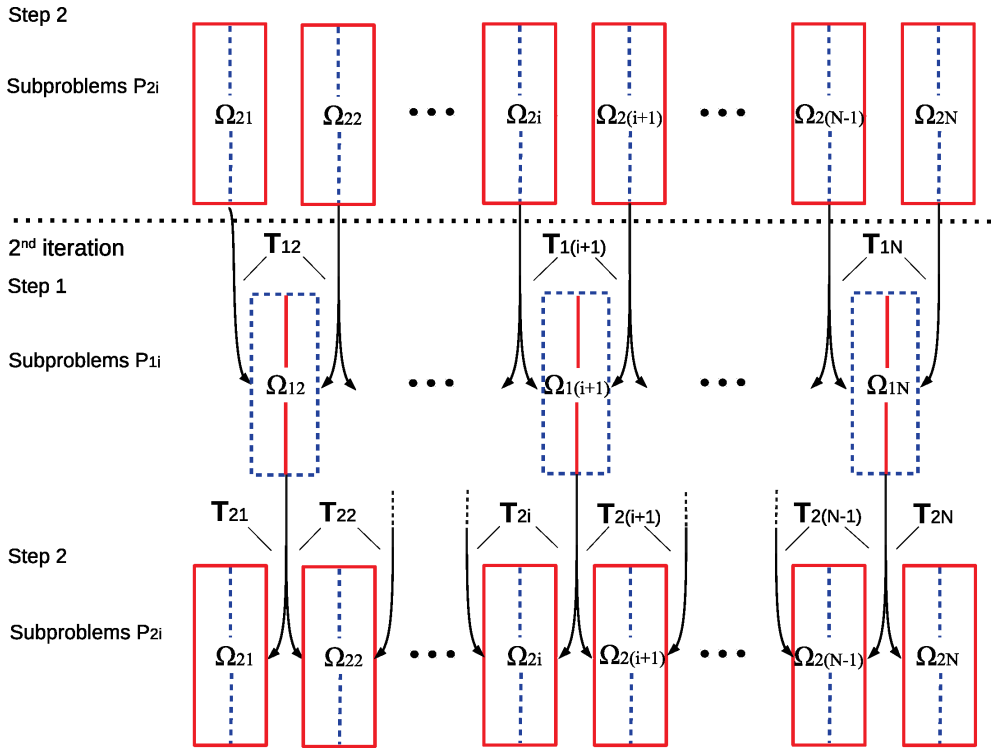

Figure 4. Decomposition flow diagram—second iteration.

It is interesting to note that the update of the solution of problem P at each step does not require adjustment or coordination among the solutions of the subproblems. This is an advantage over the case of decomposition for limit analysis, where the load parameters provided by the subproblems have to be scaled down to their common minimum. In the limit analysis subproblems, the traction vectors at the internal boundaries are scaled by the load parameter [47, 57], which is a global variable that couples the entire stress field through the equilibrium equations. Consequently, coordination among subproblems is necessary to ensure the static admissibility of the global stress field generated from the subproblem solutions.

The process is considered to converge when the improvement in the weight over an iteration falls below a preset tolerance. Because the solution at any intermediate step is feasible with respect to the target problem, a premature termination provides a conservative solution with an upper bound for the target optimal weight.

5. Numerical examples

This section illustrates the performance of the proposed domain decomposition method through a selection of plastic topology optimization problems. In all the problems treated in this section, the loading $\boldsymbol{T}$ will consist of one or more forces, denoted by F, each distributed along a length $b = 0.1$ m. The constitutive material is governed by a Tresca yield criterion with a shear strength $\bar{s} = 1$ MPa. The size of the rectangular finite element mesh will be indicated by $(n_x \times n_y)$, where n_x and n_y denote the number of columns or rows of elementary rectangles in the x and y direction, respectively. The feasibility of the optimization problem is tested before the design process by verifying that the limit load for the fully solid domain is larger than the prescribed load.

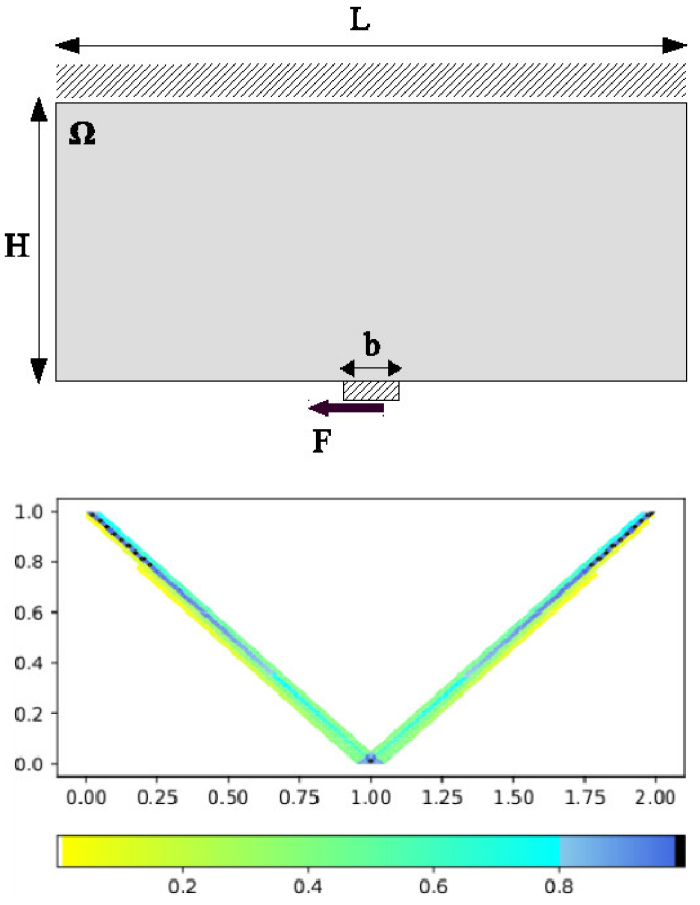

Figure 5. Short cantilever problem definition and optimal topology.

All the numerical problems, that is, the global problems and the subproblems, are treated with version 8 of the commercial solver Mosek using a laptop with a 1.8 GHz, Intel Core (i3) processor.

5.1. *The short cantilever beam subject to a single force*

The short cantilever beam problem is a classical example in the topology optimization literature (e.g., [61]). The design domain has a length $L = 2$ m and a height $H = 1$ m. It is subjected to a tangential admissible load $F = 0.09$ MN centered on its free edge and is clamped along the opposite edge, as shown in Figure 5.

The mesh chosen for the target problem has $80 \times 40 \times 4 = 12{,}800$ finite elements. An optimal weight $W_D = 0.09001$ is obtained within 15.6 s of CPU time by solving the target problem directly. As shown in Figure 5, the optimal topology is a two bar truss.

In order to examine the influence of the number of subdomains on the solution accuracy, the same target problem (based on the same target mesh) is solved with the decomposition method using partitions into $N = 2$, 4, and 8 subdomains Ω_{1i}, as described in Figure 6. The accuracy is defined by the relative error in the weight with respect to the direct solution. This measure of accuracy is justified by the lower bound property of the static LA problem.

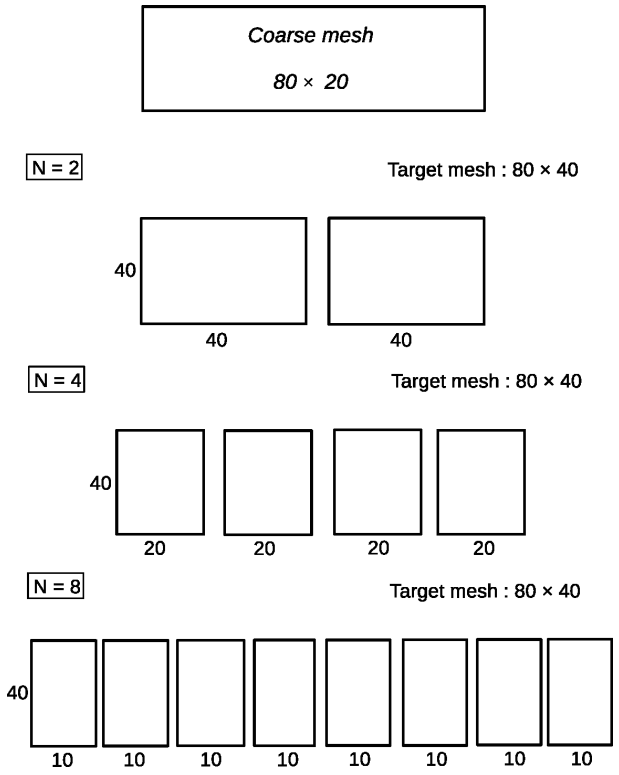

Figure 6. Domain partitions for the short cantilever problem. $N = 2$, 4, and 8.

Table 1. CPU for different partitions

N	Number of elements per subdom.	CPU (s)			
		Per subpb.	Per iter.	Coarse mesh	Target mesh
2	6400	6.29	18.87		
4	3200	3.42	23.94	6.21	15.6
8	1600	1.74	26.1		

The same initial problem is adopted for the three partitions. It is based on a coarse mesh of $80 \times 20 \times 4 = 6400$ finite elements (Figure 6), that is, half the number of elements in the target problem. Figure 7 displays the iteration histories of the weight up to the 30th iteration of the decomposition algorithm. It shows that the smaller the number of subdomains, the lower the weight, at all iterations. Moreover, convergence appears slower for $N \geq 4$. For $N = 2$, the final weight $W_2 = 0.09007$ is only 0.066% above the target, whereas for $N = 4$ and $N = 8$ it is 0.29% and 0.36%, respectively, above the target, that is, an order of magnitude less than the gap for $N = 2$.

This can be explained by the effect of fixing the internal boundary stresses during the execution of the subproblems. With a larger N, the number of internal boundaries increases and more stress variables are restrained, which results in a higher function value. The CPU times shown in Table 1 indicate that the computational effort per iteration increases moderately with the number of subdomains.

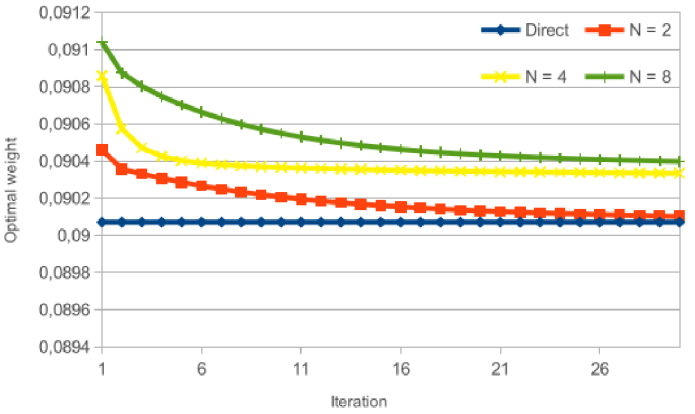

Figure 7. History of iterations of the decomposition procedure, $N = 2$, 4 and 8.

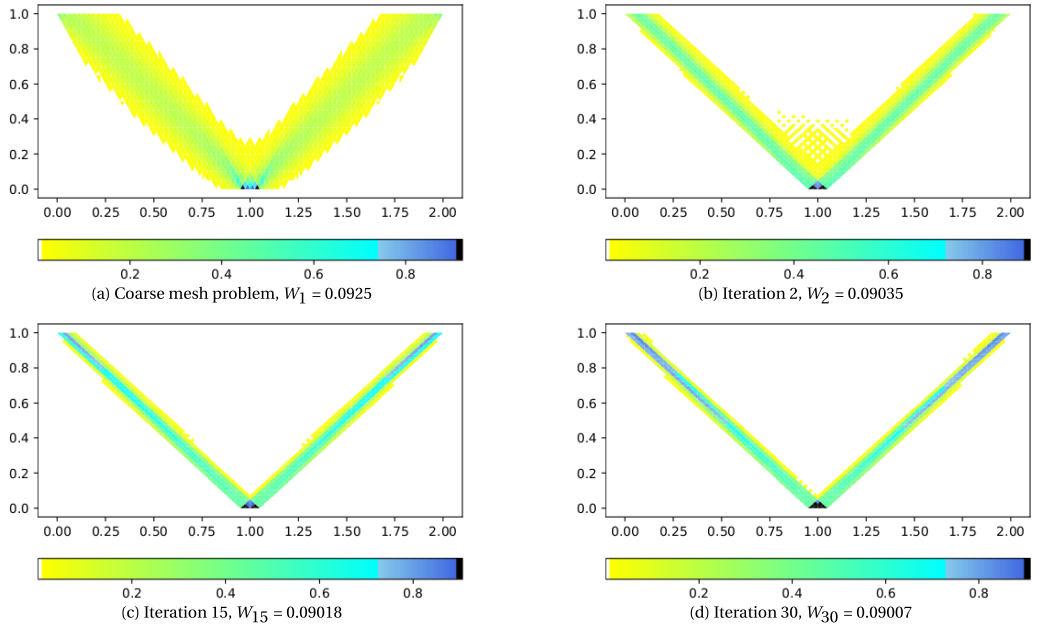

Figure 8. Designs at selected iterations using domain decomposition, $N = 2$.

The optimal topologies generated at selected iterations are presented in Figure 8 for $N = 2$. For the coarse problem, the two bars are flat with low density. As the iterations proceed, the design regularly evolves toward the optimal topology obtained by direct resolution (Figure 5).

5.2. *Short cantilever subject to multiple forces*

In this section, the topology design problem is treated using a series of increasingly fine meshes that exceed the machine capacity. The short cantilever is considered subject to multiple forces as described in Figure 9. The geometrical dimensions of the problem are $L = 3$ m, $H = 1$ m, and $b = 0.1$ m. Five equally spaced loads of magnitude $F = 0.099$ MN and spacing 0.5 m are applied

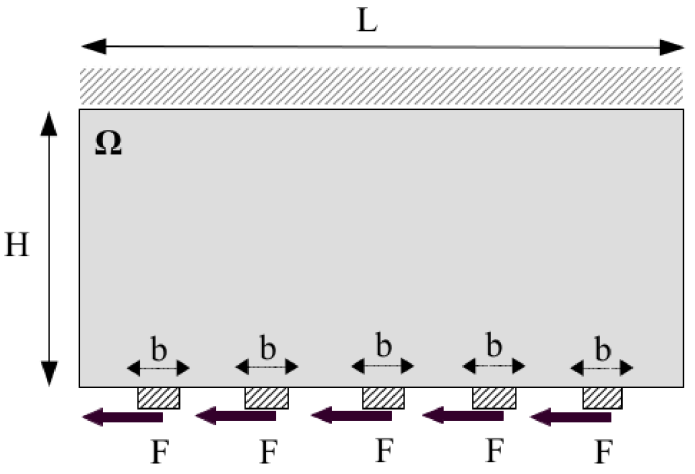

Figure 9. Short cantilever subject to multiple forces.

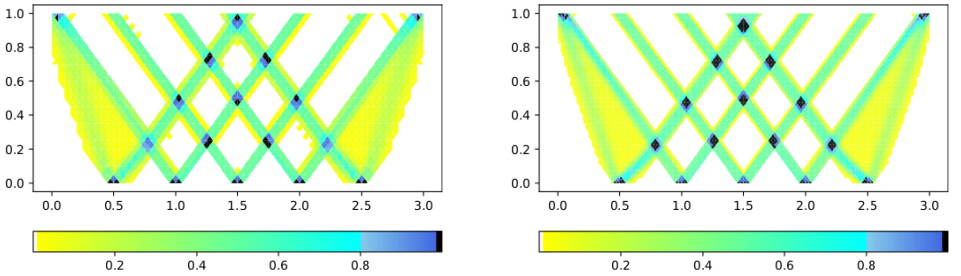

(a) (60 × 20), Weight = 0.5140

(b) (120 × 40), Weight = 0.5120

Figure 10. Short cantilever designs subject to multiple forces. Direct solutions.

at the free edge of the structure. The design domain is discretized into a series of meshes with geometrically growing size.

For the sake of objectivity of the comparison, the meshes are, in all cases, sized in similar proportions, that is, $n_x = 3n_y$, with identical finite element shapes. The topology design problem is first solved by the direct method using meshes of 4800 (= 60 × 20 × 4) and 19,200 (= 120 × 40 × 4) finite elements. Figure 10 shows the optimal topologies and optimal weights.

For meshes of more than 50,000 elements (i.e., $n_y > 64$), the direct problem could not be solved with the laptop used in this study.

The decomposition is, therefore, needed to solve larger size problems. A unique initial problem is adopted for all the series of target problems. It is the one based on the 120 × 40 mesh, that is, the largest mesh in the series that can be handled with the utilized laptop.

The domain partitions are illustrated in Figure 11. The design domain is first split into two subdomains discretized in 120 × 80 × 4 = 38,400 elements each. Larger meshes are treated using partitions into more subdomains, as indicated in Table 2.

Table 2 shows the weights obtained for the different mesh sizes. The first two results are the optimal weights obtained by direct calculation. The following weights are the results of the first iteration of the decomposition using 2, 4, and 8 subdomains. It can be noted that the finer the discretization, the better the solution of the first iteration, even with a larger number

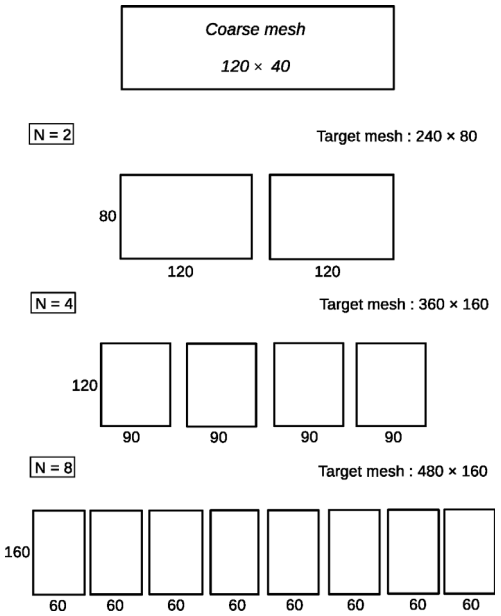

Figure 11. Decomposition into N subdomains, $N = 2$, 4, and 8.

Table 2. Optimal weights by direct and decomposition methods for different mesh sizes

Mesh	Total number of elements	Weight (direct)	N	Number of subd. elements	Weight (decomp.) (1st iter.)	CPU (s)
60×20	4800	0.5140	—	—	—	6
120×40	19,200	0.5120	—	—	—	36
240×80	76,800	—	2	38,400	0.51121	180
360×120	172,800	—	4	43,200	0.51096	420
480×160	307,200	—	8	38,400	0.51093	900

of subdomains (Figure 12). The weight drops from 0.51121 using 2 subdomains to 0.51093 for 8 subdomains, that is, an improvement of 0.055%. On the other hand, an improvement of 0.21% is achieved compared with the solution obtained using the finest mesh that can be treated directly.

5.3. *The MBB beam*

The commonly used Messerschmitt–Bolkow–Blohm (MBB) beam problem [14] illustrated in Figure 13 is considered with the geometric dimensions $L = 6$ m, $H = 1$ m. The beam is subjected to a single vertical load $F = 0.25$ MN at midspan and rests at its ends on two $e = 0.1$ m wide substrates. The prescribed load F is verified to be admissible by running the limit analysis for the fully solid beam using a mesh of $120 \times 20 \times 4 = 9600$ finite elements. For a target mesh of $960 \times 80 \times 4 = 307{,}200$ elements, the size of the direct smooth design problem exceeds the machine capacity.

Starting with the coarse mesh (120×20), the problem is solved using decomposition with a partition into eight 80×120 subdomains. The topology obtained for the target problem after one iteration of decomposition is depicted in Figure 14. In the target topology, the layouts are

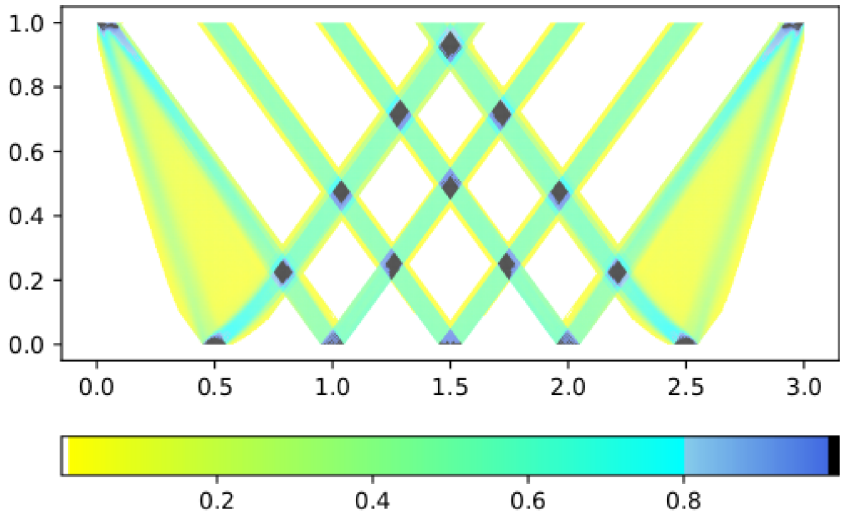

Figure 12. Optimal topology using decomposition. $N = 8$. Weight = 0.51093.

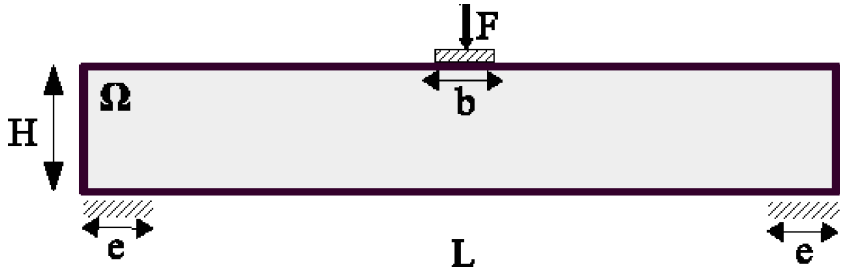

Figure 13. MBB beam problem description.

Table 3. Optimal weights by direct and decomposition methods for MBB beam

Mesh	Total number of elements	Weight (direct)	N	Number of subd. elements	Weight (decomp.) (1st iter.)	CPU (sec)
120×20	9600	1.1418	—	—	—	18.60
960×80	307,200	—	8	38,400	1.1291	825

clearer and exhibit neat compact black zones at the flanges. Comparison with the optimum design in [14] shows comparable topology except for the lower end zones. In contrast with the designs in Figure 14, the topology in [14] exhibits a continuous bottom flange that is connected to the supports which are modeled as rollers. This dissimilarity is explained by the difference in the adopted support conditions. Table 3 shows the optimal weight and the CPU time for the coarse mesh problem and the first iteration of the decomposition. A 1.1% gain in weight is achieved at the first iteration.

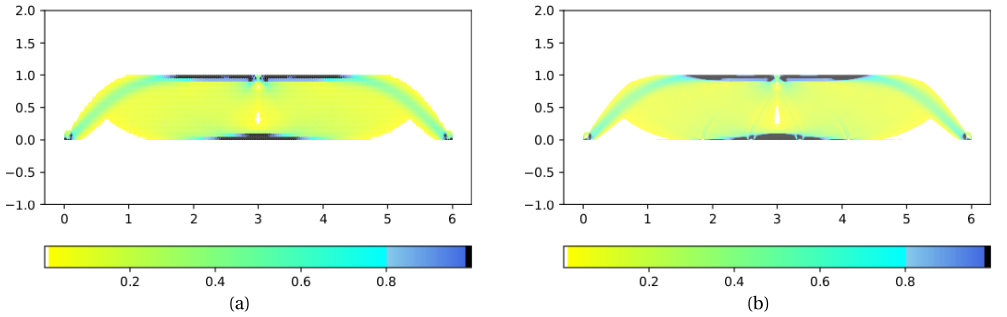

Figure 14. MBB beam final topology. (a) Coarse mesh, (b) target mesh after first iteration.

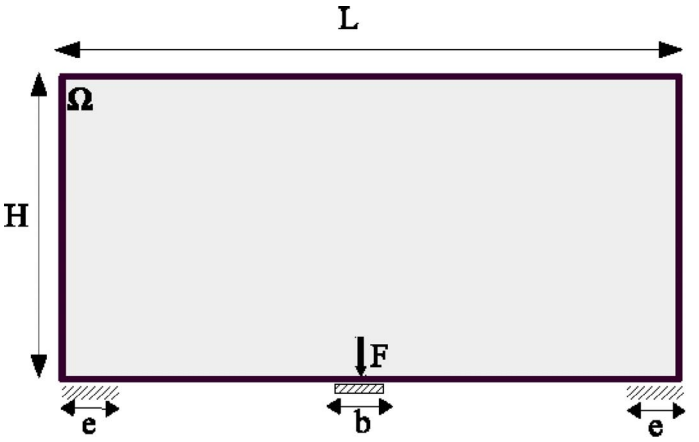

Figure 15. Mitchell truss problem description.

5.4. *The Mitchell truss*

The classical Mitchell truss problem defined in [62] is described in Figure 15. The design domain has a length $L = 2$ m and a height $H = 1$ m. It is supported at the lower ends by two substrates of width $e = 0.1$ m. The smooth optimum topology is sought for the plastic structure subject to a vertical load $F = 0.25$ MN located at the middle of the domain base. With a target finite element mesh of $320 \times 160 \times 4 = 204{,}800$ elements, the design cannot be performed directly. The decomposition is carried out starting with a coarse mesh of 80×40 and a partition into $N = 8$ subdomains of 160×40.

The final topology is depicted in Figure 16. Table 4 displays the minimum weight and the CPU time relative to the starting problem and the first iteration of the decomposition. A single iteration resulted in a 0.4% weight reduction and visibly no change in the design compared with the solution of the coarse mesh problem.

5.5. *The medium cantilever beam*

In this example, the decomposition is tested on a significantly large problem. The medium length cantilever beam problem defined in [63], and described in Figure 17, is considered with the dimensions $L = 2$ m and $H = 1$ m. The prescribed 50 kN vertical load is applied at the lower part of the free edge. The target mesh counts $640 \times 320 \times 4 = 819{,}200$ finite elements and the

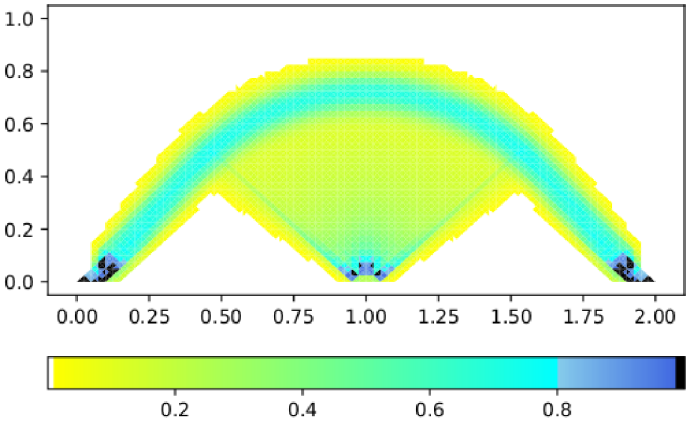

Figure 16. Mitchell truss final topology after 1 iteration of decomposition.

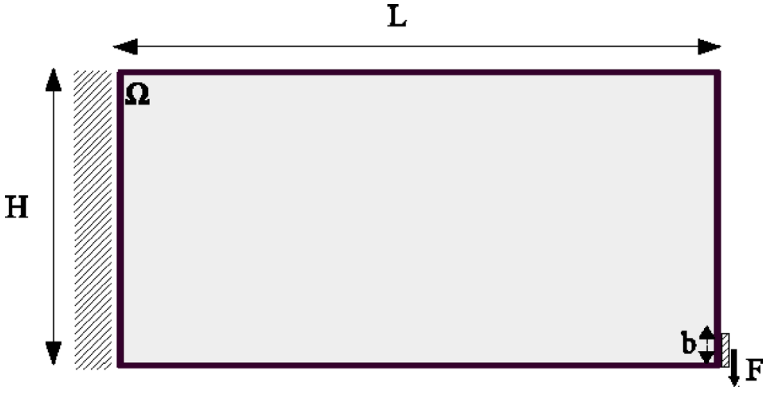

Figure 17. Medium cantilever beam problem description.

Table 4. Optimal weights for Mitchell truss

Mesh	Total number of elements	Weight (direct)	N	Number of subd. elements	Weight (decomp.) (1st iter.)	CPU (s)
80×40	12,800	0.30032	—	—	—	23.86
320×160	204,800	—	8	25,600	0.29901	425

integrated design optimization problem has nearly 8 million variables. For an i3 processor, this is a considerably large numerical problem which necessitates decomposition. With a coarse mesh of 160×80, the starting problem nears the machine capacity. The domain is partitioned into $N = 8$ subdomains of 80×320. The optimum solutions of the coarse design problem and the first iteration of the decomposition are shown in Figure 18. The target topology exhibits well-defined isodensity zones in the web of the beam, whereas the coarse design shows a smoothly graded density field.

The weight and the CPU time relative to the initial and target problems are given in Table 5. A 0.6% gain in weight is achieved after one iteration of the decomposition.

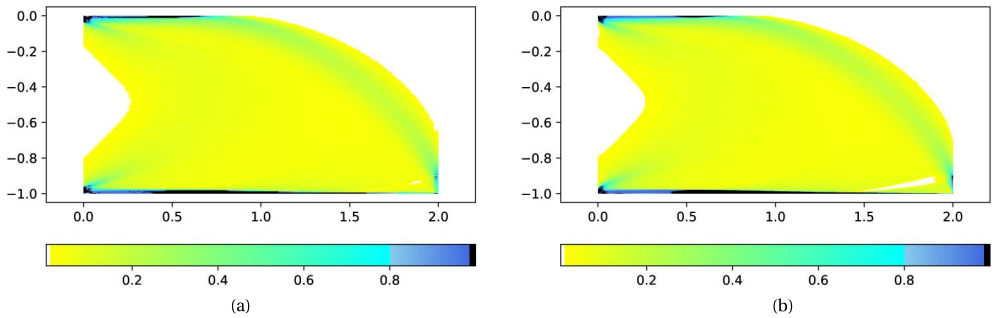

Figure 18. Medium cantilever final topologies. (a) Initial problem, (b) first iteration of decomposition.

Table 5. Optimal weights for medium cantilever beam problem

Mesh	Total number of elements	Weight (direct)	N	Number of subd. elements	Weight (decomp.) (1st iter.)	CPU (min)
160×80	51,200	0.18589	—	—	—	145
640×320	819,200	—	8	102,400	0.18474	3300

6. Conclusion

A domain decomposition strategy is proposed for solving large-scale, smooth topology optimization problems beyond the available computational and storage capacities. It is developed for plastic design, using a stress-based integrated limit analysis and design approach. The limit analysis is precisely appropriate for plastic design as it circumvents the computational burden associated with path dependence. Integrating the design with the static limit analysis is confirmed to be suitable for decomposition as it preserves the appealing mathematical structure and properties of the underlying limit analysis problem. Specifically, (i) convexity is favorable for global convergence of the decomposition strategy, (ii) the lower bound property of the static limit analysis formulation implies that the intermediate solutions generated during the decomposition process provide admissible designs, (iii) the absence of a stress–strain law and kinematic response variables in the formulation reduces the coupling between substructures, and (iv) the separable (or node-wise separable) form of the objective and constraint functions is favorable for decomposition of the mathematical problem. Moreover, the sparse conic quadratic programming form of the design problems and subproblems allows highly efficient solution using primal–dual, interior point methods.

The presented decomposition method consists of a converging sequence of topology design subproblems of smaller size than that of the target design problem. It involves a repeated alternation of two overlapping partitions of the material domain. At each iteration, an independent topology optimization subproblem is associated with each subdomain. The stresses at the interfaces between subdomains are updated at each iteration. The iterative process is initialized by solving a coarse design problem.

A remarkable advantage of the method is that it achieves a substantial drop in weight at the first iteration. Numerical tests show that the weight systematically reduces to less than 0.1% above the direct solution at the first iteration of the decomposition, which is not frequent in decomposition methods. Moreover, the lower bound character of the static approach implies

that premature termination, even as early as the first iteration, provides a feasible, that is, conservative, near optimal solution that is usable in approximate design or in a practical context. In contrast, the convergence to the optimal solution is slow in general. It is noted, however, that the process converges faster with fewer subdomains. This suggests that a combination of coarse and fine partitions analogous to the multigrid strategies could be a viable path to speed up convergence to the solution when the computing resources are limited.

While the partitions were carried out here along a single direction, the present findings should conceptually hold for partitions in two directions. This will be verified upon implementation of the extension in two directions. The assumption of infinitesimal strain constitutes a definite limitation of the limit analysis based method. However, some of the assumptions made are not restrictive. For instance, the choice of a Tresca yield criterion is not necessary for the methodology, which is applicable with other standard convex criteria such as von Mises. The fixed support conditions may be modified to allow frictional or smooth sliding for a more meaningful comparison with benchmark problems. The plane strain assumption is not necessary, nor is the 2D restriction. The 3D extensions of the integrated LA and design formulation and decomposition strategy visibly present no conceptual gap. Finally, as the smooth design problem is a component in many 0–1 topology optimization strategies, the proposed decomposition method can be incorporated in these strategies to solve large-scale plastic 0–1 topology design problems.

References

[1] G. Costa, M. Montemurro, J. Pailhès, "NURBS hyper-surfaces for 3D topology optimization problems", *Mech. Adv. Mater. Struct.* **28** (2021), no. 7, p. 665-684.

[2] K.-F. Seitz, J. Grabe, "Three-dimensional topology optimization for geotechnical foundations in granular soil", *Comput. Geotech.* **80** (2016), p. 41-48.

[3] P. G. Coelho, J. B. Cardoso, P. R. Fernandes, H. C. Rodrigues, "Parallel computing techniques applied to the simultaneous design of structure and material", *Adv. Eng. Softw.* **42** (2011), no. 5, p. 219-227.

[4] M. P. Scardaoni, M. Montemurro, "A general global-local modelling framework for the deterministic optimisation of composite structures", *Struct. Multidiscipl. Optim.* **62** (2020), p. 1927-1949.

[5] J. Sobieszczanski-Sobieski, B. B. James, A. R. Dovi, "Structural optimization by multilevel decomposition", *AIAA J.* **23** (1985), no. 11, p. 1775-1782.

[6] T. Woo, L. Schmit, "Decomposition in optimal plastic design of structures", *Int. J. Solids Struct.* **17** (1981), no. 1, p. 39-56.

[7] B. H. V. Topping, A. I. Khan, *Parallel Finite Element Computations*, Saxe-Coburg Publications, Edinburgh, 1996.

[8] L. S. Lasdon, *Optimization Theory for Large Systems*, Courier Corporation, USA, 2002.

[9] T. Borrvall, J. Petersson, "Large-scale topology optimization in 3D using parallel computing", *Comput. Methods Appl. Mech. Eng.* **190** (2001), no. 46–47, p. 6201-6229.

[10] A. Mahdavi, R. Balaji, M. Frecker, E. M. Mockensturm, "Topology optimization of 2D continua for minimum compliance using parallel computing", *Struct. Multidiscipl. Optim.* **32** (2006), no. 2, p. 121-132.

[11] Z. Kammoun, H. Smaoui, "A direct approach for continuous topology optimization subject to admissible loading", *C. R. Méc.* **342** (2014), no. 9, p. 520-531.

[12] Z. Kammoun, "A formulation for multiple loading cases in plastic topology design of continua", *C. R. Méc.* **344** (2016), no. 10, p. 725-735.

[13] Z. Kammoun, M. Fourati, H. Smaoui, "Direct limit analysis based topology optimization of foundations", *Soils Found.* **59** (2019), no. 4, p. 1063-1072.

[14] M. A. Herfelt, P. N. Poulsen, L. C. Hoang, "Strength-based topology optimisation of plastic isotropic von Mises materials", *Struct. Multidiscipl. Optim.* **59** (2019), no. 3, p. 893-906.

[15] J. Fin, L. A. Borges, E. A. Fancello, "Structural topology optimization under limit analysis", *Struct. Multidiscipl. Optim.* **59** (2019), no. 4, p. 1355-1370.

[16] Z. Kammoun, H. Smaoui, "A direct method formulation for topology plastic design of continua", in *Direct Methods for Limit and Shakedown Analysis of Structures* (P. Fuschi, A. Pisano, D. Weichert, eds.), Springer, Cham, 2015, p. 47-63.

[17] H. Smaoui, Z. Kammoun, "Convergence of the direct limit analysis design method for discrete topology optimization", *Optim. Eng.* (2020), https://doi.org/10.1007/s11081-020-09543-6.

[18] A. Lyamin, S. Sloan, "Lower bound limit analysis using non-linear programming", *Int. J. Numer. Methods Eng.* **55** (2002), no. 5, p. 573-611.
[19] A. Lyamin, S. Sloan, "Upper bound limit analysis using linear finite elements and non-linear programming", *Int. J. Numer. Anal. Methods Geomech.* **26** (2002), no. 2, p. 181-216.
[20] J. Fin, L. A. Borges, E. A. Fancello, "Structural topology optimization under limit analysis", *Struct. Multidiscipl. Optim.* **59** (2019), no. 4, p. 1355-1370.
[21] M. P. Bendsøe, O. Sigmund, "Material interpolation schemes in topology optimization", *Arch. Appl. Mech.* **69** (1999), no. 9, p. 635-654.
[22] P. Duysinx, M. P. Bendsøe, "Topology optimization of continuum structures with local stress constraints", *Int. J. Numer. Methods Eng.* **43** (1998), no. 8, p. 1453-1478.
[23] M. Bruggi, "On an alternative approach to stress constraints relaxation in topology optimization", *Struct. Multidiscipl. Optim.* **36** (2008), no. 2, p. 125-141.
[24] C. Le, J. Norato, T. Bruns, C. Ha, D. Tortorelli, "Stress-based topology optimization for continua", *Struct. Multidiscipl. Optim.* **41** (2010), no. 4, p. 605-620.
[25] D. Yang, H. Liu, W. Zhang, S. Li, "Stress-constrained topology optimization based on maximum stress measures", *Comput. Struct.* **198** (2018), p. 23-39.
[26] C. Fleury, H. Smaoui, "Convex approximation strategies in structural optimization", in *Discretization Methods and Structural Optimization—Procedures and Applications* (H. A. Eschenauer, G. Thierauf, eds.), Lecture Notes in Engineering, vol. 42, Springer, Berlin, Heidelberg, 1989, p. 118-126.
[27] K. Svanberg, "A class of globally convergent optimization methods based on conservative convex separable approximations", *SIAM J. Optim.* **12** (2002), no. 2, p. 555-573.
[28] G. Xu, C. Gengdong, "Epsilon-continuation approach for truss topology optimization", *Acta Mech. Sin.* **20** (2004), no. 5, p. 526-533.
[29] Y. M. Xie, G. P. Steven, "A simple evolutionary procedure for structural optimization", *Comput. Struct.* **49** (1993), no. 5, p. 885-896.
[30] M. P. Bendsøe, N. Kikuchi, "Generating optimal topologies in structural design using a homogenization method", *Comput. Methods Appl. Mech. Eng.* **71** (1988), no. 2, p. 197-224.
[31] G. Strang, R. V. Kohn, "Optimal design in elasticity and plasticity", *Int. J. Numer. Methods Eng.* **22** (1986), no. 1, p. 183-188.
[32] G. Costa, M. Montemurro, J. Pailhès, "Minimum length scale control in a NURBS-based SIMP method", *Comput. Methods Appl. Mech. Eng.* **354** (2019), p. 963-989.
[33] R. Zakhama, M. Abdalla, H. Smaoui, Z. Gürdal, "Multigrid implementation of cellular automata for topology optimization", in *First International Conference on Multidisciplinary Design and Applications* (Besançon, France), 2007.
[34] G. Costa, M. Montemurro, J. Pailhès, "A 2D topology optimisation algorithm in NURBS framework with geometric constraints", *Int. J. Mech. Mater. Des.* **14** (2018), no. 4, p. 669-696.
[35] K. Maute, S. Schwarz, E. Ramm, "Adaptive topology optimization of elastoplastic structures", *Struct. Optim.* **15** (1998), no. 2, p. 81-91.
[36] M. Wallin, V. Jönsson, E. Wingren, "Topology optimization based on finite strain plasticity", *Struct. Multidiscipl. Optim.* **54** (2016), no. 4, p. 783-793.
[37] G. Zhang, L. Li, K. Khandelwal, "Topology optimization of structures with anisotropic plastic materials using enhanced assumed strain elements", *Struct. Multidiscipl. Optim.* **55** (2017), no. 6, p. 1965-1988.
[38] J. Salençon, *Yield Design*, John Wiley & Sons, 2013.
[39] D. C. Drucker, W. Prager, "Soil mechanics and plastic analysis or limit design", *Q. Appl. Math.* **10** (1952), no. 2, p. 157-165.
[40] A. Gvozdev, "The determination of the value of the collapse load for statically indeterminate systems undergoing plastic deformation", *Int. J. Mech. Sci.* **1** (1960), no. 4, p. 322-335.
[41] G. Maier, "Quadratic programming and theory of elastic-perfectly plastic structures", *Meccanica* **3** (1968), no. 4, p. 265-273.
[42] J. Lysmer, "Limit analysis of plane problems in soil mechanics", *J. Soil Mech. Found. Div.* **96** (1970), no. 4, p. 1311-1334.
[43] J. Pastor, "Analyse limit determination numerique de solutions statistique completes, Application au talus vertical", *J. Mech. Appl.* **2** (1978), p. 167-196.
[44] E. D. Andersen, C. Roos, T. Terlaky, "On implementing a primal-dual interior-point method for conic quadratic optimization", *Math. Program.* **95** (2003), no. 2, p. 249-277.
[45] H. Smaoui, "Finite element limit load analysis by the static approach using nonlinear programming", in *Computing in Civil Engineering*, ASCE, 1994, p. 1936-1943.
[46] J. Pastor, T.-H. Thai, P. Francescato, "Interior point optimization and limit analysis: an application", *Int. J. Numer. Methods Biomed. Eng.* **19** (2003), no. 10, p. 779-785.

[47] Z. Kammoun, F. Pastor, H. Smaoui, J. Pastor, "Large static problem in numerical limit analysis: a decomposition approach", *Int. J. Numer. Anal. Methods Geomech.* **34** (2010), no. 18, p. 1960-1980.
[48] K. Anoukou, F. Pastor, P. Dufrenoy, D. Kondo, "Limit analysis and homogenization of porous materials with Mohr–Coulomb matrix. Part I: Theoretical formulation", *J. Mech. Phys. Solids* **91** (2016), p. 145-171.
[49] R. Sun, J. Yang, "Axisymmetric adaptive lower bound limit analysis for Mohr–Coulomb materials using semidefinite programming", *Comput. Geotech.* **130** (2021), article no. 103906.
[50] K. Krabbenhoft, L. Damkilde, "A general non-linear optimization algorithm for lower bound limit analysis", *Int. J. Numer. Methods Eng.* **56** (2003), no. 2, p. 165-184.
[51] R. T. Haftka, "Integrated nonlinear structural analysis and design", *AIAA J.* **27** (1989), no. 11, p. 1622-1627.
[52] H. Smaoui, L. Schmit, "An integrated approach to the synthesis of geometrically non-linear structures", *Int. J. Numer. Methods Eng.* **26** (1988), no. 3, p. 555-570.
[53] D. Yang, H. Liu, W. Zhang, S. Li, "Stress-constrained topology optimization based on maximum stress measures", *Comput. Struct.* **198** (2018), p. 23-39.
[54] J. F. Benders, "Partitioning procedures for solving mixed-variables programming problems", *Numer. Math.* **4** (1962), p. 238-252.
[55] B. Maar, V. Schulz, "Interior point multigrid methods for topology optimization", *Struct. Multidiscipl. Optim.* **19** (2000), no. 3, p. 214-224.
[56] F. Pastor, E. Loute, "Limit analysis decomposition and finite element mixed method", *J. Comput. Appl. Math.* **234** (2010), no. 7, p. 2213-2221.
[57] J. J. Muñoz, N. Rabiei, A. Lyamin, A. Huerta, "Computation of bounds for anchor problems in limit analysis and decomposition techniques", in *Direct Methods for Limit States in Structures and Materials*, Springer, 2014, p. 79-99.
[58] J. Salençon, "Théorie des charges limites: poinçonnement d'une plaque par deux poinçons symétriques en déformation plane", *C. R. Méc. Acad. Sci. Paris* **265** (1967), p. 869-872.
[59] F. Alizadeh, D. Goldfarb, "Second-order cone programming", *Math. Program.* **95** (2003), no. 1, p. 3-51.
[60] A. Mosek, "The MOSEK optimization software", 2020, Online at, http://www.mosek.com.
[61] Q. Q. Liang, Y. M. Xie, G. P. Steven, "Optimal topology selection of continuum structures with displacement constraints", *Compos. Struct.* **77** (2000), no. 6, p. 635-644.
[62] G. Allaire, M. Schoenauer, *Conception Optimale de Structures*, vol. 58, Springer, 2007.
[63] M. Abdi, I. Ashcroft, R. Wildman, "Topology optimization of geometrically nonlinear structures using an evolutionary optimization method", *Eng. Optim.* **50** (2018), no. 11, p. 1850-1870.